FLOODPLAIN ROUGHNESS MAPPING SYNERGY: LIDAR AND SPECTRAL REMOTE SENSING

M. Straatsma

Utrecht University, Faculty of Geosciences, Department of Physical Geography, PO Box 80115, 3508 TC, Utrecht, The Netherlands

KEY WORDS: Roughness mapping, data fusion, multispectral data, airborne laser scanning data, object-oriented classification, floodplain vegetation

ABSTRACT:
Floodplain roughness parameterization is one of the key elements of hydrodynamic modeling of river flow, which is directly linked to safety level estimation of lowland fluvial areas. Necessary input parameters are median grain size for unvegetated areas, vegetation density for forest and vegetation height and density for herbaceous vegetation. This paper presents a method for spatially distributed roughness parameterization, in the entire floodplain by fusion of CASI multispectral data with airborne laser scanning (ALS) data. The method consists of two stages: (1) image segmentation of the fused dataset and classification into the most important land cover classes (overall accuracy = 81 percent, and (2) determination of hydrodynamic surface characteristics for each class separately. In stage two, a lookup table provides numerical values that enable roughness computation for water, sand, paved area, meadows and built-up areas. For the other classes, forest and herbaceous vegetation, ALS data enabled spatially detailed analysis of vegetation height and density. The vegetation density of forest is mapped using a calibrated regression model. Herbaceous vegetation was further subdivided in single trees and non-woody vegetation. Single trees were delineated using a novel iterative cluster merging method, and their height is predicted (R^2 = 0.41). The vegetation density of single trees was determined identically to forest Vegetation height and density of non-woody herbaceous vegetation was determined using calibrated regression models. This method provides hydrodynamic modelers with a highly automized procedure for roughness mapping with much spatial detail.

1. INTRODUCTION

Hydrodynamic modelling is essential for river management, not only to calculate local water levels for the current design discharge, but also to assess the effect of future climate change and ecological river restoration measures. In addition to surface topography, hydrodynamic roughness of the floodplain surface is the key parameter of hydrodynamic models. It is a function of the vegetation height and density in case of vegetated areas, and of grain size and bed form shape in case of unvegetated areas (Baptist, 2005). For vegetated areas, a distinction is made between submerged and emergent vegetation with respect to the water level during peak flow. Emergent vegetation is described by vegetation density, which is the projected plant area in the direction of the flow per unit volume (Petryk and Bosmajian, 1975; Figure 1). Considering vegetation as cylindrical elements, this equals the product of number of stems or stalks per unit area multiplied by the average stem diameter. Roughness of submerged vegetation is determined by vegetation height and density (Baptist, 2005). To provide hydrodynamic modelers with reliable input, the spatial and temporal distribution of surface characteristics is needed. This asks for monitoring methods that can cover large floodplain areas, and are detailed and fast.

Traditional methods to map roughness patterns within the floodplain are based on visual interpretation and manual classification of vegetation units derived from aerial photographs, as applied for the lower Rhine floodplains (Van Velzen et al., 2003). This is a time consuming method that does not allow to document within-class variation of vegetation roughness. In literature, many studies report successful and accurate mapping of natural vegetation using multispectral or hyperspectral remote sensing data (Mertes, 2002). Recently, spectral information has been combined with height information in vegetation classification schemes (e.g., Dowling and Accad (2003). Even though the spatial resolution and the level of detail of the classification increases with these classifications, still a lookup table should be used to convert the vegetation classes to vegetation structure values. Airborne laser scanning (ALS), however, enables direct extraction of vegetation structural characteristics such as forest vegetation height, biomass, basal area, and leaf area index (Lefsky et al., 2002). Moreover, vegetation height of low vegetation was also mapped for crops, and grassland (Cobby et al., 2001; Mason et al., 2003). Straatsma and Middelkoop (in press) give an overview of studies that extract hydrodynamically relevant vegetation characteristics from ALS data. However, the noise level of ALS data is around 5 cm for flat unvegetated areas (Davenport et al., 2000; Hopkinson et al., 2004), which makes extraction of surface properties of sandy surfaces or meadows difficult if not impossible.

Therefore, our aim is to use a combination of spectral and ALS remote sensing data to map floodplain surface characteristics relevant for hydrodynamic modelling. The new method consisted of two stages; (1) image segmentation and classification into the main hydrodynamically relevant land cover types, and (2) determination of roughness input parameters of these land cover types using a lookup table and direct analysis of vegetation structure.

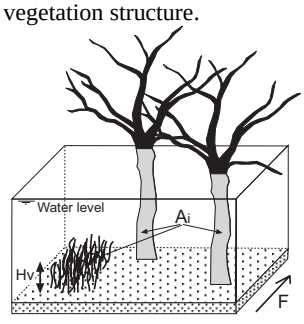

Figure 1. Hydrodynamic parameters; vegetation density (m^2m^{-3}) the sum of projected plant areas (A) in the direction of the water flow (F) per unit volume (cube), and vegetation height (Hv)

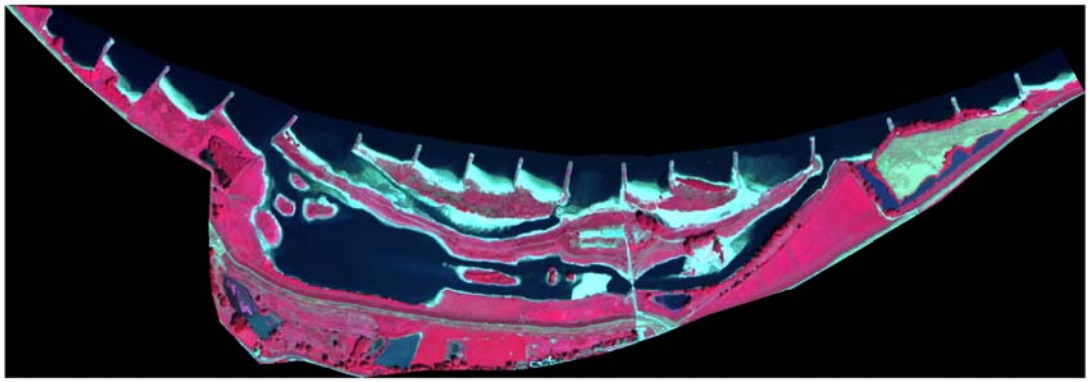

Figure 2: Gamerense Waard floodplain false colour CASI image (band 732)

2. MATERIALS AND METHODS

2.1 Study area

This study uses airborne remote sensing data collected over the Gamerense Waard (GW) floodplain, situated on the left bank of the embanked river Waal, the main distributary of the River Rhine in the Netherlands. The GW floodplain is essentially flat, except for the embankments and eroding shorelines of the side channels. Land cover is a combination of meadows, open water and nature areas that partly consisted of forests (figure 2). In addition to the forest patches, also individual trees of variable age were present. All vegetation was in winter condition when the laser data was acquired and in summer condition at the moment of CASI data collection. The typical inundation depth is 3 m during periods of high river discharge, but it might rise up to 5 m in case of extreme flood events.

2.2 Field data

A field campaign in June 2004 yielded information on important properties of 213 single trees in the study area, north of the western side channel. Location, height and circumference of these trees were measured to establish a regression model for tree height as a check for the single tree delineation from ALS data. Locations of the trees were determined using a dGPS in real time kinematics mode. Tree height was measured using a levelling beacon.

2.3 Remote sensing data

2.3.1 CASI multispectral image: On July 11 2003, a multispectral image was acquired with the airborne multispectral scanner: CASI, Compact Airborne Spectral Imager. The system is an along-track scanner and acquires data in 10 channels between 400 and 900 nm, programmable at 2-nm spectral intervals (Lillesand and Kiefer, 1994). For this flight campaign, 10 bands were programmed, of which six in the near infra red to optimize discrimination of various vegetation types. The image was georectified by the data vendor. Table 1, and 2 give the specific settings for this flight. It turned out that the georeferencing by the vendor of the CASI image was of insufficient quality match the *spectral* data acquired together with the ALS data. Therefore, additional image registration was carried out using rubber sheeting (Hartmann et al., 2004).

2.3.2 Airborne laser scanning: The ALS data of the Gameren floodplain were acquired using the FLI-MAP II system mounted on a helicopter. FLI-MAP, Fast Laser Imaging and Mapping Airborne Platform, is a small-footprint, first pulse, scanning laser range finder combined with a dGPS and an Inertial Navigation System (INS) for positioning. Table 3 summarizes the characteristics. In 2003, the FLI-MAP system consisted of two laser range finders, resulting in combined pulse rate of 20 kHz. The two scanners were facing 7° forward and backward to decrease the amount of occlusion in built-up areas. Additionally, FLI-MAP II has acquired true-colour, high-resolution photographs simultaneously with the laser data. A georeferenced photo-mosaic was supplied together with the laser data, which served to match the CASI data to the ALS data. On March 11 2003, the FLI-MAP II system was deployed over the GW floodplain. The data vendor filtered the ALS data and labelled points as either ground or non-ground points.

Table 1 Metadata for the CASI mission

Acquisition date	11-7-2003
Acquisition time	11:45
Flying height	1700 m
Strip width	1046 m
Pixel size at nadir	2 m
No. of bands	10

Table 2 Spectral properties of the CASI image

Band no.	Band middle (nm)	Band width (nm)	Description
1	450	20	Blue
2	552	10	Green
3	670	10	Red
4	700	10	NIR[a]
5	710	10	NIR
6	740	10	NIR
7	750	10	NIR
8	780	10	NIR
9	820	10	NIR
10	865	10	NIR

[a] NIR = Near Infra Red

Table 3 Meta data for the laser scanning mission

Acquisition date	11-03-2003
Scan angle	± 30°
Scan line orientation	± 7°
No. of sensors	2
Pulse rate	2*10 kHz
Flying height	80 m
Point density	75 m^{-2}

2.4 Data processing

To make optimal use of the information in the laser-derived point data and spectral gridded data, a two-stage method was used to derive roughness input values covering the whole floodplain. In the stage 1, an object-oriented classification was carried out to discriminate between land cover types. A supervised classification was carried out to discriminate between water, sand, meadow, herbaceous vegetation and forest. In stage 2, specific methods were applied to each of the land cover types to estimate the input for roughness computation.

2.4.1 Stage 1: Segmentation and classification into land cover types: The commercial software package Ecognition (Definiens, 2003) was used to compute segments from the image to derive image objects. The ALS data was fused with the CASI data into a multi-source dataset aiming at floodplain land cover classification. In a pre-processing step a Digital Surface Model (DSM) was computed from the ALS data that described the vegetation height of the top of the canopy. Therefore, the height above the DTM, the point height, was computed for each non-ground point. The gridded DSM, with the same cell size as the CASI data, was computed as the 95 percentile of the point heights in each cell. Table 4 gives the weights assigned to the individual layers during the segmentation. The weight of the ALS layer was set to the summed weights of the spectral layers.

Table 4. Segmentation weights for the individual layers of the multi source dataset.

Layer	Weight
CASI 1	2
CASI 2	3
CASI 3	2
CASI 4	1
CASI 5	1
CASI 6	2
CASI 7	2
CASI 8	1
CASI 9	1
CASI 10	1
ALS	16

Different scale settings were tested, and visual inspection showed that a scale parameter of 10 resulted in small segments appropriate for the vegetation distribution as observed in the field. Furthermore, a weight of 0.9 was given to information contained in the eleven layers, and a weight of 0.1 was used for shape.

The supervised classification of image objects was carried out using linear discriminant analysis (Davis, 1986), based on a training data set of 217 randomly selected image objects. The selected objects were classified based on visual inspection of the CASI and ALS data, field knowledge, and the vegetation maps of Van Gennip and Bergwerff (2002). A minimum of 15 objects were classified in each class. The following classes were discerned based on their different roughness and spectral attributes: water, wet sand, dry sand, paved area, meadow, herbaceous vegetation, dry herbaceous vegetation, forest, and built-up area. Wet sand and dry sand have different spectral values, but the same roughness, and these classes can therefore be merged after classification, just like herbaceous vegetation and dry herbaceous vegetation. The accuracy of the classification was tested using a leave-one-out cross validation. This procedure leaves one image object out of the training dataset and predicts its class using the remaining reference data. The results are presented in an error matrix, and summarized by the overall accuracy, and the kappa statistic was computed (Lillesand and Kiefer, 1994).

2.4.2 Segmenting herbaceous vegetation into single trees and non-woody vegetation

The class herbaceous vegetation consists of a wide range of vegetation types since it is the succession stage between meadow and forest. Therefore it might include non-woody vegetation as well as young trees. Vegetation structure estimation of non-woody herbaceous vegetation is not valid at the location of the trees. Therefore a single tree delineation method has to segment the laser point cloud into woody and non-woody segments.

Different tree delineation methods are available literature. Persson et al. (2002), for example, created digital canopy models, smoothed at different scales. Alternatively, single tree delineation was applied on raw laser data, having the advantage that no data points were lost due to gridding (Morsdorf et al., 2004). For floodplain vegetation, we tested this k-means clustering method of Morsdorf et al. (2004). The results were unsatisfactory, since the clustering resulted often in two cluster centroids for large trees, while adjacent small trees were not identified as a separate cluster. Therefore, the method was adapted with cluster merging using iterative cross-section analysis. This method generates many clusters based on seed points that over-represent large trees. Cluster are subsequently merged depending on the cross-sections between the clusters. Details of the method are described below, and illustrated in figure 3.

Firstly, low (< 1.5 m) and isolated vegetation points (< 2 neighbours in a 1 m neighbourhood) were excluded from further analyses, since these often represented herbaceous vegetation. Secondly, a k-means cluster analyses was carried out using local maxima as seed points (figure 3a). Local maxima were identified in the point cloud by assigning the highest hit in a local window with a 0.7 m radius to each point in a moving window.

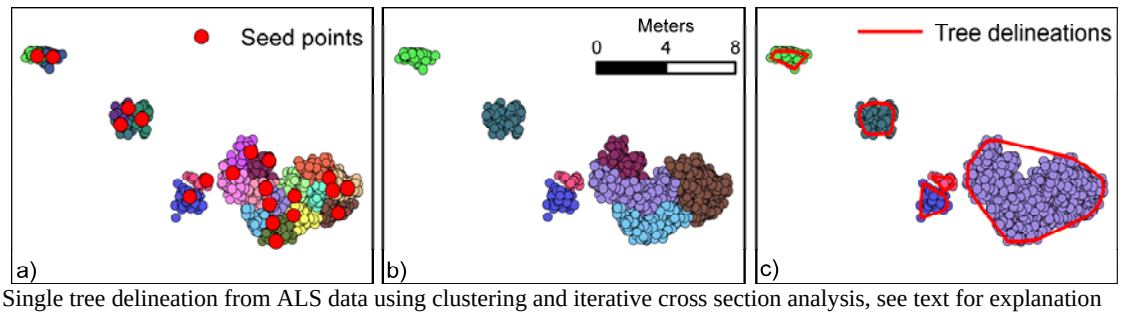

Figure 3 Single tree delineation from ALS data using clustering and iterative cross section analysis, see text for explanation

This radius was selected because it was about the average tree radius of 0.66 m as observed in the field. In case the vegetation height of the point was the same as the highest point in the local window, the point was labelled as a local maximum. Thirdly, the cross sections between cluster maxima were classified as referring to either one or two trees depending on whether or not an open space existed of 25 cm in the cross section. Finally, clusters were merged iteratively until all cross sections satisfied the specified condition (figure 3b). The 2D convex hull of final merge gives the polygon that describes the outline of a tree (figure 3c).

2.4.2 Stage 2: Determination of hydrodynamic surface characteristics: The second stage consisted of class-specific methods to estimate the hydrodynamic surface characteristics. Therefore, vegetation density should be extracted from the ALS data for forest patches, vegetation height and density should be mapped for herbaceous vegetation (separated into single trees and non-woody vegetation), and a lookup table should be used for the other classes; meadow, unvegetated area, and built-up area. The lookup table was needed since no method was available to extract the hydrodynamically relevant surface characteristics of these classes from either ALS of CASI data.

Forest
Straatsma (2005) used the percentage index (PI) to map the hydrodynamic vegetation density of floodplain forest. The PI computes the percentage of laser hits that fall within the height range that could be inundated by the water, and is defined as:

$$PI_{h1-h2} = \frac{1}{h2-h1} * \frac{N_{h1-h2}}{N_{tot}} \quad (1)$$

in which $N_{h1\text{-}h2}$ is the number of points between height 1 and 2 above the forest floor, N_{tot} is the total number of points in the field plot including canopy and ground surface points. The height interval for PI was set to 0.5 to 2.5 m. The PI is sensitive to the number of laser pulses that were emitted of which no return was detected by the receiver. However, a check for these so-called invalid points showed that the number of invalid points for the GW dataset was less than one promille. The regression model of (Straatsma, in prep.) was used to predict the hydrodynamic vegetation density (Dv):

$$Dv = 1.36 * PI + 0.008 \ (R^2 = 0.66, N = 22) \quad (2)$$

Herbaceous vegetation
Vegetation height of a delineated tree is derived from a regression model based on manually linked tree clusters to field derived tree height estimates. The automatic linking of clusters to trees was not satisfactory, probably because of the time difference of acquisition between the laser data and the field data. The vegetation height of the trees were assigned to the polygon, which was converted to a grid in a final step to ensure a similar output for all land cover classes.

The key issue in vegetation structure mapping of non-woody herbaceous vegetation is point labelling as ground or vegetation, since the thin stalks of herbs in senescence are difficult to detect by ALS. Therefore, the point labelling of herbaceous vegetation was carried out following Straatsma and Middelkoop (in prep.). They modelled the histogram of the residual vertical distance between the point height and the DTM. This point height distribution is considered as the sum of the noise distribution of ground points and a uniform distribution of the vegetation points. The point of maximum upward concavity, the inflection point, is used as a threshold for labelling. All points above the threshold were labelled as vegetation. The height of the inflection point changes due to differences in noise levels, or flight strips that do not match exactly. Therefore, this procedure of point labelling was carried out separately for each image object segmented in stage 1, while points within the tree polygons were excluded. Vegetation height (Hv) and density (Dv) were computed from regression models determined for the same area in a previous study. They are valid for vegetation heights in the order of 0.3 to 2 m and vegetation densities in the order of $3 * 10^{-4}$ to 0.7 m^2/m^3 (Straatsma and Middelkoop, in prep.).

$$Hv = 1.47 * D_{95} + 0.28 \ (R^2 = 0.78, N = 31) \quad (3)$$
$$Dv = 1.18 * PI + 0.03 \ (R^2 = 0.66, N = 43) \quad (4)$$

where D_{95} is the 95 percentile of the vegetation points, and PI is the Percentage Index computed over the height of the vegetation. This resulted in a spatially distributed map of non-woody vegetation height and density.

2.4.3 Other land cover classes: The land cover classes water, sand, paved, meadow, and built-up area were assigned a lookup value. Both water and sand should be assigned a median grain size only as a roughness parameter. However, depending on hydrodynamic conditions sub aqueous dunes will develop. Also the median grain size may vary spatially over the distributaries of the River Rhine.

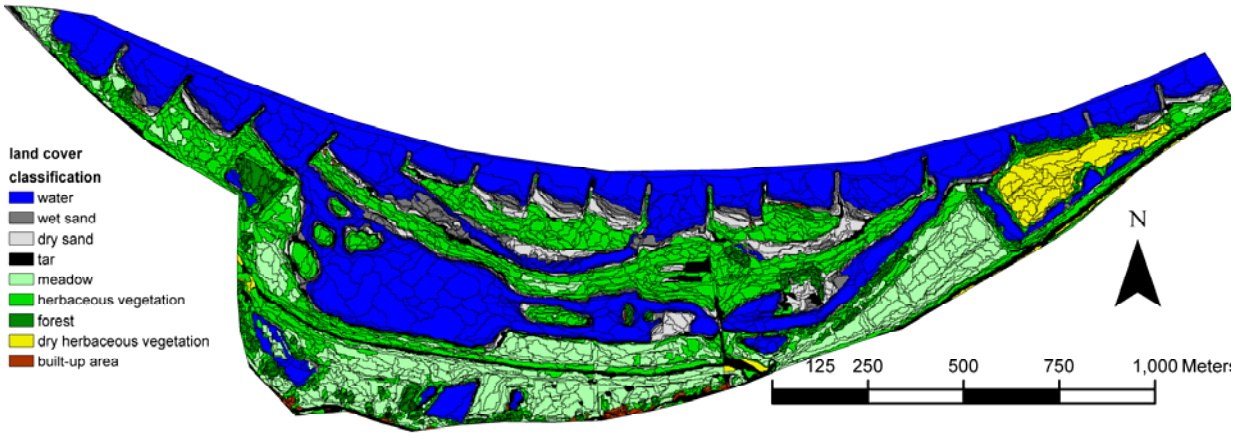

Figure 4 Classified land cover map using object oriented classification

Table 5: Error matrix resulting from leave-one-out cross validation on 217 reference data

	Water	Wet sand	Dry sand	Paved	Meadow	Herbs	Forest	Dry herbs	Built-up	row total	Users accuracy
Water	**30**	0	0	0	0	0	0	0	0	30	1.00
Wet sand	1	**10**	1	2	0	3	0	0	0	17	0.59
Dry sand	0	0	**13**	0	0	0	0	0	0	13	1.00
Paved	0	3	1	**10**	0	0	0	0	0	14	0.71
Meadow	0	2	0	0	**25**	8	0	0	1	36	0.69
Herbs	1	0	0	1	11	**45**	2	2	0	62	0.73
Forest	0	0	0	0	0	1	**17**	0	0	18	0.94
Dry herbs	0	0	0	1	0	0	0	**13**	0	14	0.93
Built-up	0	0	0	1	0	0	0	0	**14**	15	0.93
Column total	32	15	15	15	36	57	19	15	15		
Prod. accuracy	0.94	0.67	0.87	0.67	0.69	0.79	0.89	0.87	0.93		

3. RESULTS

The results of the classification of image objects is shown in figure 4. The error matrix is given in table 5. The largest errors are related to the distinction between meadow and herbaceous vegetation. The overall accuracy is 81 percent and the kappa statistic is 0.77. After joining wet and dry sand into a single class sand and herbs and dry herbs into herbs, the overall accuracy increases slightly to 82 percent, and the kappa statistic to 0.78

The field campaign yielded information of the position, height and circumference of 213 individual trees. Tree heights ranged between 0.5 to 7.5 m, and the average was 3.6 m. The spatial pattern of the tree distribution is similar to the trees extracted from the ALS data. Vegetation height of the individual trees was estimated using a regression model derived from the field observations (figure 7):

$$H_{max} = 0.7 * H_{max.laser} + 1.6 \ (R^2 = 0.41, N = 86) \quad (5)$$

The vegetation height and density maps of herbaceous vegetation is presented in figure 5a, and 5b. The vegetation density map of forest is given in figure 5c. Differences in vegetation density within a single forest patch are clearly visible just below the ‘c’ in figure 5c. With these input maps, the hydrodynamic roughness can be computed together with the flood water levels. However, the resulting map will also display the effect of the differences in water depth due to topographic elevation differences. Roughness computation is outside the scope of this paper.

4. DISCUSSION

This paper presents a new method for automatic mapping of input for floodplain roughness parameterization using a combination of multispectral data, and airborne laser scanning data. The ALS data enabled the accurate computation of vegetation height and density of herbaceous vegetation and forest. This approach gets around the need to use a lookup table to characterize the vegetation structure of these classes. However, ALS is unsuitable to distinguish between land cover classes such as water, paved areas, beaches or meadows. The integrated use of spectral remote sensing with ALS is a suitable solution to separate these land cover classes.

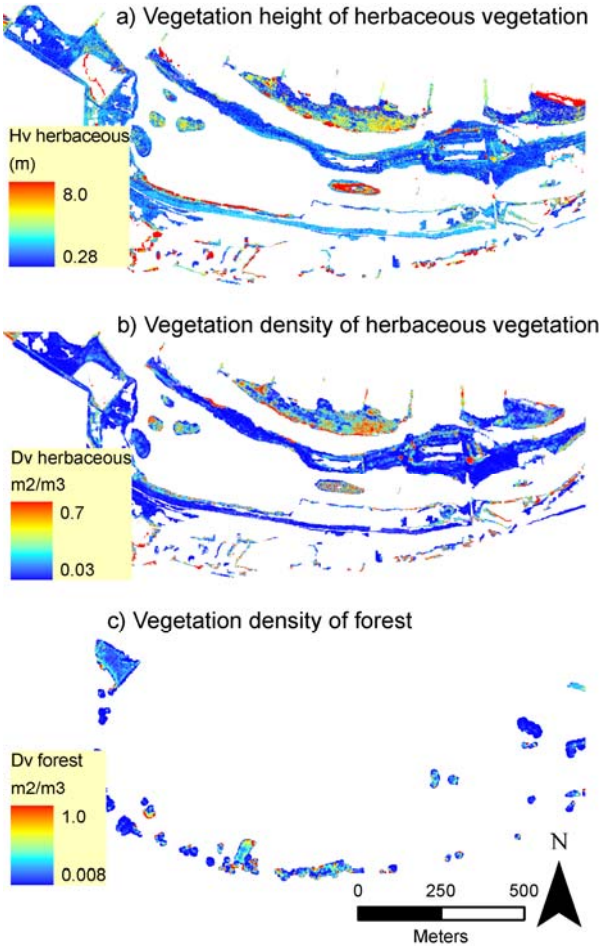

Figure 5: a) vegetation height of herbaceous vegetation b) vegetation density of herbaceous vegetation, c) Vegetation density of forest

Classification of the image objects using a linear discriminant analysis proved successful given the overall accuracy of 81 percent. Linear discriminant analysis has the advantage that it can account for many parameters in the discriminant function, since it assumes the variance per layer to be equal for each group. This limits the size of the training dataset, which is especially important when an a-select sampling strategy is applied in which classes with a low occurrence are not well represented. The distinction between herbaceous vegetation and meadows proved the most challenging

vegetation classes to distinguish with a user accuracy of around 70 percentage. This is particularly important, since large parts of the floodplain consist of these two land cover types. It is advised to focus on this distinction in future studies.

The single tree delineation using the iterative cross section analysis in this study used only a single attribute of the cross section, namely whether or not an open space existed of 25 cm in the cross section. Alternatively, more features of the cross section could be taken into account that characterize the shape and position of the cross section by using a discriminant analysis to classify the cross sections. This makes the new procedure highly flexible for different vegetation types and laser point densities. The explained variance of the regression model for tree height ($R^2 = 0.41$) is relatively low when compared to other studies (Perssonet al., 2002). The reason might be the time delay between the laser campaign and the field inventory of 1.5 year.

5. CONCLUSION

This paper describes a new method to derive hydrodynamically relevant surface characteristics. The fusion of multispectral data and airborne laser scanning data provides an accurate tool for detailed and accurate floodplain roughness assessment. The classification of image objects into nine classes showed an overall accuracy of 81 percent. Water, unvegetated areas, meadows, and built-up areas are best described by using a lookup table, since no roughness parameter could be extracted from either data source. The spatial distribution of vegetation density of forest, computed using the Percentage Index ($R^2 = 0.66$), matched the patterns as observed in the field. Vegetation height and density of herbaceous vegetation were computed using regression models that were calibrated for the specific laser data and vegetation type ($R^2 = 0.78$ for vegetation height, $R^2 = 0.51$ for vegetation density). Moreover, a new single tree delineation method is presented. This method first performs a clustering using local maxima as seed points. Subsequently, clusters are merged based on the attributes of the cross section between the clusters. The final result of the combined mapping methods is a highly detailed map stack of surface properties of the floodplain that can serve as input to hydrodynamic models.

REFERENCES

Baptist, M.J., 2005. Modelling floodplain biogeomorphology, Delft technical University, Delft, 195 pp.

Cobby, D.M., Mason, D.C. and Davenport, I.J., 2001. Image processing of airborne scanning laser altimetry data for improved river flood modeling. *ISPRS Journal of Photogrammetry and remote sensing*, 56(121-138).

Davenport, I.J., Bradbury, R.B., Anderson, G.R.F., Hayman, J.R., Krebs, J.R., Mason, D.C., Wilson, J.D. and Veck, N.J., 2000. Improving bird population models using airborne remote sensing. *International Journal of Remote Sensing*, 21(13,14): 2705-2717.

Davis, J.C., 1986. *Statistics and data analyses in geology*. John Wiley & sons, New York, 646 pp.

Definiens Imaging, 2003. eCognition user guide. Definiens Imaging GmbH, Münich.

Dowling, R. and Accad, A., 2003. Vegetation classification of the riparian zone along the Brisbane River, Queensland, Australia, using light detaiction and ranging (lidar) data and forward looking digital video. Canadian Journal of Remote Sensing, 29(5): 556-563.

Hartmann, R., Brügelmann, R. and Bollweg, A., 2004. Vegetatieclassificatie uit laser en optische RS data. AGI/0109/GAR002, AGI, Delft.

Lefsky, M.A., Cohen, W.B., Parker, G. and Harding, D., 2002. Lidar remote sensing for ecosystem studies. *Bioscience*, 52(1): 19-30.

Lillesand, T.M. and Kiefer, R.W., 1994. *Remote sensing and image interpretation*. John Wiley & sons, New York, 750 pp.

Mason, D.C., Cobby, D.M., Horrit, M.S. and Bates, P., 2003. Floodplain friction parameterization in two-dimensional river food models using vegetation heights derived from airborne scanning laser altimetry. *Hydrological Processes*, 17: 1711-1732.

Mertes, L.A.K., 2002. Remote sensing of riverine landscapes. *Freshwater Biology*, 47: 799-816.

Morsdorf, F., Meier, E., Kotz, B., Itten, K.I., Dobbertin, M. and Allgower, B., 2004. LIDAR-based geometric reconstruction of boreal type forest stands at single tree level for forest and wildland fire management. *Remote Sensing of Environment*, 92(3): 353-362.

Persson, Å., Holmgren, J. and Söderman, U., 2002. Detecting and measuring individual trees using an airborne laser scanner. *Photogrammetric Engineering & Remote Sensing*, 68(9): 925-932.

Petryk, S. and Bosmajian, G., 1975. Analysis of flow through vegetation. *Journal of hydraulics divisions*, 101: 871-884.

Straatsma, M.W., 2005. Quantitative mapping of hydrodynamic vegetation density of floodplain forests using airborne laser scanning. In: G. Vosselman and C. Brenner (Editors), ISPRS workshop laser scanning 2005. ISPRS, Enschede.

Straatsma, M.W., in prep. Quantitative mapping of hydrodynamic vegetation density of floodplain forests using airborne laser scanning.

Straatsma, M.W. and Middelkoop, H., submitted. Extracting structural characteristics of herbaceous floodplain vegetation for hydrodynamic modeling using airborne laser scanner data. International Journal of Remote Sensing.

Straatsma, M.W. and Middelkoop, H., in press. Airborne laser scanning as a tool for lowland floodplain vegetation monitoring. *Hydrobiologia*.

Van Gennip, B. and Bergwerff, J., 2002. Ecotopen- en struweelkartering Gamerensche Waard 2002 (in Dutch). MD-GAE-2002.37, RIZA, Lelystad.

Van Velzen, E.H., Jesse, P., Cornelissen, P. and Coops, H., 2003. Flow friction of vegetation in floodplains part 1 (in Dutch). 2003.028, RIZA, Arnhem.